Available online at www.sciencedirect.com
SCIENCE DIRECT®
International Journal of Heat and Mass Transfer 48 (2005) 3256–3260
International Journal of HEAT and MASS TRANSFER
www.elsevier.com/locate/ijhmt

Technical Note

Mass transfer in plane and square ducts

S.B. Beale *

National Research Council, Montreal Road, Ottawa, Ont., Canada K1A 0R6

Received 26 July 2004; received in revised form 8 February 2005

Abstract

A numerical mass transfer analysis for plane and square duct geometries for developing and fully-developed scalar transport with laminar flow is described. A methodology for prescribing stream-wise periodic scalar boundary conditions under conditions of constant-transformed-substance state, is detailed. The solution to the fully-developed mass transfer problem is presented in terms of driving force, blowing parameter and normalised conductance. A suitably-defined polarisation factor is shown to be functionally equivalent to the former. The data compress onto a single curve with good correspondence to the 1-D convection–diffusion solution, except for high rates of wall injection or suction.

Keywords: Mass transfer; Ducts; Computational fluid dynamics

1. Introduction

There are a number of situations where mass transfer in ducts is an important consideration, e.g. in fuel cells and membrane separation devices. Computational fluid dynamics (CFD) can solve the governing transport equations, however a problem arises; when large numbers of channels are present, an enormous geometric mesh is required. One solution is to replace diffusive terms with rate terms, according to,

$$j'' = -\Gamma \partial\phi/\partial y|_w = g(\phi_w - \phi_b) \quad (1)$$

where ϕ_w and ϕ_b are wall and bulk values of mass fraction (or enthalpy). Variations in the conductance, g, as a function of geometry and mass transfer rate, $\dot{m}''$, need to be accounted-for: In contrast to external problems, these are not well-characterised for internal flows, in the literature. Three possible approaches are (a) theoretical analysis, (b) fine-scale numerical calculation, or (c) experimental data/empirical correlation. Cases (a) and (b) are considered here. Let it be supposed [1] that

$$\dot{m}'' = gB \quad (2)$$

where $B = (\phi_b - \phi_w)/(\phi_w - \phi_t)$ is a driving force and ϕ_t is the value of ϕ at the transferred-substance or t-state. Alternatively in terms of blowing parameter, b

$$\dot{m}'' = g^* b \quad (3)$$

where g^* is the value of g as $\dot{m}'' \to 0$.

In the present work, mass transfer in ducts is analysed using a numerical integration scheme. The scope of the problem is confined to Fickean diffusion, for laminar flow with constant properties, negligible dissipation, and Lewis number of unity. Soret (and Dufour) thermo-diffusion effects are neglected. Most theoretical hydrodynamic analyses are for plane ducts, Fig. 1(a). Berman [2] obtained a solution for fully-developed flow in a plane channel with injection/suction at both walls. Injection at only one wall, Fig. 1(b), was considered in [3,4] and

* Tel.: +1 613 993 3487; fax: +1 613 941 1571.
E-mail address: steven.beale@nrc-cnrc.gc.ca

0017-9310/$ - see front matter
doi:10.1016/j.ijheatmasstransfer.2005.02.037

Nomenclature

C	source term coefficient
D_h	hydraulic diameter (m)
g	conductance $\Gamma\partial\phi/\partial y\|_w/(\phi_b-\phi_w)$ (kg/m^{2}s)
j''	rate of transfer of ϕ/m^2
L	length (m)
u	stream-wise velocity (m/s)
v	cross-wise velocity (m/s)
V	source term value
H	height, half-height (m)
$\dot{m}''$	rate of mass transfer (kg/m^{2}s)
p	pressure (Pa)
S	source term, $C(V-\phi_P)$

Greek symbols

ϕ	scalar variable
Γ	exchange coefficient (kg/ms)
μ	viscosity (kg/ms)
ρ	density (kg/m^3)

Non-dimensional numbers

B	driving force $(\phi_b-\phi_w)/(\phi_w-\phi_t)$
b	blowing parameter $\dot{m}''/g^*$
c_f	friction factor $\mu\partial u/\partial y\|_w/\frac{1}{2}\rho u_b^2$
Sh/Nu	Sherwood/Nusselt number gD_h/Γ
Pe	Peclet number $\rho D_h v_w/\Gamma$
Pe_w	Wall Peclet number $\frac{1}{4}\rho D_h v_w/\Gamma$
Re	Reynolds number $\rho D_h u/\mu$
Re_w	Wall Reynolds number $\frac{1}{4}\rho D_h v_w/\mu$
Sc/Pr	Schmidt/Prandtl number Γ/μ
Φ	polarisation $(\phi_w-\phi_b)/(\phi_b-\phi_t)$
ξ	non-dimensional distance $\frac{1}{3}(v_w/u_b(0))(4x/D_h)Pe_w^2$

Superscripts

*	for zero mass transfer
′	per unit length
.	per unit time

Subscripts

0	inlet condition
b	bulk
cell	cell
t	transferred-substance state
w	wall

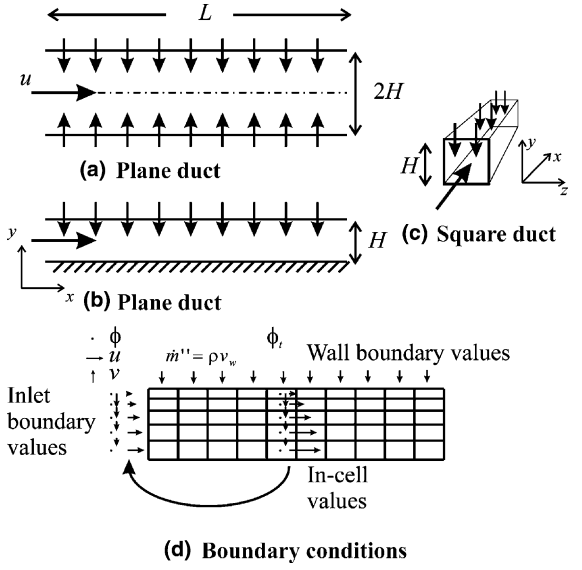

Fig. 1. Boundary conditions for three problems considered in this study.

elsewhere. Numerical solutions were reported in [5,6], a review of flow in porous ducts is found in [7]. Work on mass/heat transfer have also been primarily concerned with planar geometry, often for suction; of interest in membrane science. Sherwood et al. [8–10] considered mass transfer for reverse osmosis based on [2] (for mathematical details see Appendix A). Numerical studies of heat and mass transfer have also been reported [11–19]. In this study, calculations are performed for the cases shown in Fig. 1(a–c). The equations solved are of the form [20],

$$\mathrm{div}(\rho\vec{u}\phi)=\mathrm{div}\Gamma\mathrm{grad}\phi+\dot{S}''' \tag{4}$$

These are integrated to obtain finite-volume equations having the form, $\sum a_{nb}(\phi_{nb}-\phi_P)+S=0$, where ϕ_{nb} is the 'neighbour' value to cell 'P' [20]. Source terms are linearised; $S=C(V-\phi_P)$, where C is a 'coefficient' and V is a 'value'. Three types of wall boundary conditions are anticipated: (i) prescribed ϕ_w, (ii) prescribed ϕ_t, (iii) fixed flux, j''. For (i) $V=\phi_w$, the coefficient, C, is computed using an 'exponential scheme'. For case (ii) with injection, a linearised source, $C=\dot{m}''A_{cell}$, $V=\phi_t$ is prescribed; however for suction; a fixed source $\dot{S}=\dot{m}''A_{cell}(\phi_t-\phi_P)$ is set, to avoid the creation of negative C-coefficients [20]. Often $\phi_t=1$; however for membrane transport with incomplete rejection $\phi_t<1$; and for heterogeneous chemical reactions $-\infty\leqslant\phi_t\leqslant\infty$. Previous authors [11–14,19] considered heat/mass transfer problems for fixed wall-value or flux. Typically, the value/flux, will not be constant, due to convection, and the constant t-state prescription, as given here, is reasonable under many circumstances. Note that as $\dot{m}''\to 0$, constant t-state approaches constant wall flux condition.

Three inlet conditions were considered: (a) constant scalar $\phi = \phi_0$, (b) prescribed velocity profiles [2] for case (1), and (c) 'periodic' boundary conditions, where values at $x = L/2$ are back-substituted as illustrated in Fig. 1(d); u-values are scaled by $u_b(0)/u_b(L/2)$. For scalar transport, it is presumed that $(\phi - \phi_w)/(\phi_b - \phi_t)$ is constant, and inlet values of ϕ, are computed from those at $x = L/2$, and then scaled to yield the prescribed bulk inlet value [21],

$$\phi(0, y) = c_1\phi(L/2, y) + c_2 \tag{5}$$

where $c_1 = (\phi_b(0) - \phi_w(0))/(\phi_b(L/2) - \phi_w(L/2))$ and $c_2 = \phi_w(0) - c_1\phi_w(L/2)$. The upstream wall value must be computed, $\phi_w(0) = (\phi_b(0) + B\phi_t)/(1 + B)$, where $B = B(L/2)$. At $x = L$, a constant pressure was prescribed. The code PHOENICS was used to perform the calculations.

2. Results and discussion

Fig. 2 is a comparison of the present work with Sherwood et al. [8] for developing scalar transport, fully-developed flow, $Pe_w = -2$, -3.7 and -14.8. The results are presented in terms of a polarisation, Φ, defined by,

$$\Phi = (\phi_w - \phi_b)/(\phi_b - \phi_t) \tag{6}$$

as a function of non-dimensional distance, ξ, defined in the nomenclature. Also shown are 'fully-developed' results based on Eq. (5). These are asymptotic solutions in the limit, $|\xi| \gg 0$. For large negative Pe_w (strong suction) this condition may never be reached.

Sherwood et al. defined a concentration polarisation for the considered phase as the quantity $\phi_w/\phi_b - 1$. This is equivalent to Eq. (6) with $\phi_t = 1$ for the transferred phase: however there are many situations where $\phi_t \neq 1$; reverse-osmosis with incomplete rejection, heterogeneous chemical reactions, and sensible heat transfer where ϕ_t is the ambient (enthalpy/temperature) value. Under these circumstances Φ, as defined in Eq. (6), is invariant. It can be shown that $1/B + 1/\Phi = -1$, so the polarisation and driving force are functionally equivalent. Tests confirmed that regardless of the choice of ϕ_t; identical B and Φ characteristics were obtained.

Fig. 3 shows g/g^*, as a function of B and b, for fully-developed scalar transport, Fig. 1(a)–(c). For case (3), these are based on an average value of ϕ_w. The solid lines are the 1-D convection–diffusion solution. An estimate for g may be made, given the 1-D solution and g^*, obtained from $Sh^* = 8.23$, 5.38, and 2.71, respectively [22]. NB: for scalar transport $b = 4Pe_w/Sh^*$ where $Sh^* = g^*D_h/\Gamma$, and $Pe_w = Re_w/Sc$, and $Re_w = \rho D_h v_w/4\mu$. Fig. 4 shows Φ and B as a function of b. The approximate solution of Sherwood et al, $\Phi = \frac{1}{3}Pe_w^2$ is appropriate only for suction. There is good agreement with the 1-D solution except at high values of $b \gg 0$, where the 1-D solution underpredicts B. Similarly $\Phi = \exp(-b) - 1$ overpredicts Φ for $b \ll 0$. The data are compressed towards $B = -1$ for strong suction, and $\Phi = -1$ for blowing. Plots of $\ln(1 + B)$ or $\ln(1 + \Phi)$ vs b, remove this bias and display a linear form, for $-1 \leqslant b \leqslant +1$. Outside this

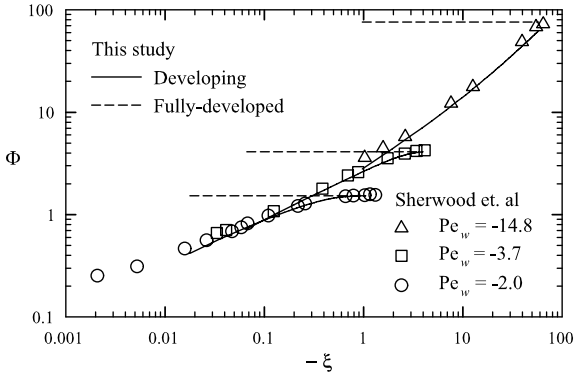

Fig. 2. Developing scalar polarisation for case (a).

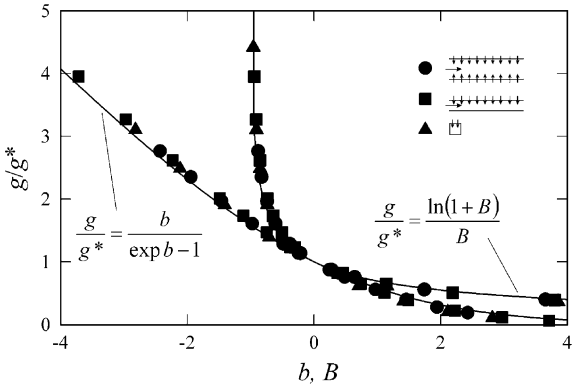

Fig. 3. Fully-developed normalised conductance as a function of blowing parameter and driving force.

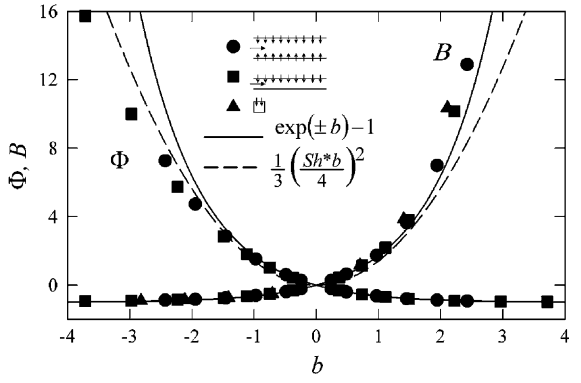

Fig. 4. Fully-developed driving force and polarisation as a function of blowing parameter.

region non-linearities are observed; However, the three data sets all fall onto a single characteristic curve of B vs b. If, however there are variations in the Sc/Pr, significant departures from this characteristic are anticipated.

The main-flow Re varies continuously as u_b changes with x, however a 'fully-developed' hydrodynamic regime is observed downstream, where $c_f = \tau_w/\frac{1}{2}\rho u_b^2(x)$ is constant. NB: With $c_f^* = a/Re$ and $g/\rho u_b = c_f/2$, it follows that $b = 8Re_w/a$. Fig. 5 shows c_f as a function of b, for momentum transfer. The c_f/c_f^* data do not compress on a single characteristic curve. The straight line is obtained from Berman's [2] linear perturbation solution (see Appendix A). For case (a) injection; $\frac{1}{2}\rho u_b^2$ and hence pressure gradient increase, however c_f/c_f^* decreases, since $\partial u/\partial y$ must decrease at both walls. The profile is qualitatively similar to g/g^* for scalar transport, Fig. 3. Cases (b) and (c) are different: for (b) a decrease in $\partial u/\partial y$ at one wall is accompanied by an increase at the opposite wall, and c_f/c_f^* increases for sufficiently strong injection. This behaviour is pronounced for case (c) where momentum transfer occurs at all four walls, and was noted by Yuan et al. [19] who included reversible (pressure) losses in their definition of c_f. Although there are large apparent changes in c_f/c_f^*, the blowing parameter for momentum transfer, b, is generally very small. Comparison of pressure coefficient, u and v-velocity profiles with [2] were quite satisfactory [23]. The assumption of constant downstream pressure will lead to localised errors as the blowing parameter, b, becomes large in magnitude, and secondary (cross-wise) pressure gradients arise in addition to stream-wise gradients. These errors are local and do not affect the results presented, as the downstream region was discarded.

Standard mass transfer techniques are well suited to this class of internal-flow problem, despite pressure variations, heat and mass transfer problems are to be considered identical for the problem Fig. 1(a). However, heat transfer boundary conditions may be different for cases (b) and (c) in that mass transfer occurs at only one boundary, whereas heat transfer may occur simultaneously at the other walls [19,22] if the thermal conductivity of the solid walls is sufficiently large and there are external temperature gradients.

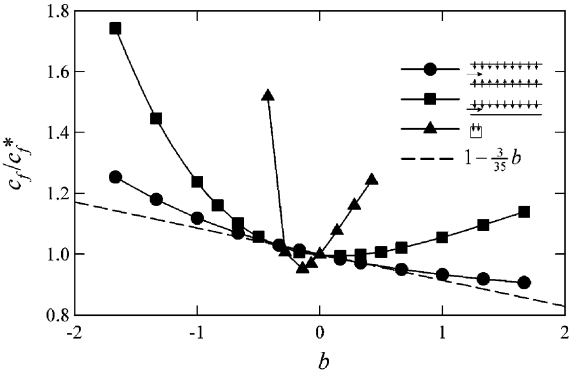

Fig. 5. Fully-developed normalised friction coefficient as a function of blowing parameter.

3. Conclusions

Numerical calculations were performed for fluid flow, and scalar transport in the passages of plane and square ducts under constant t-state boundary conditions. Both developing and fully-developed inlet conditions were considered. The back-substitution process allows fully-developed flow for arbitrary geometry to be prescribed. The effects of injection are to decrease scalar transfer conductance, while increasing the pressure gradient. Suction has the opposite effects. The influence on the friction coefficient is more complex; suction always increases friction, whereas injection may either decrease or increase friction, depending on geometry and boundary conditions. A fully-developed situation is always attained except for large negative Pe_w. Heat/mass transfer conductances and friction coefficients are significantly affected by mass transfer at the wall. An appropriate independent variable for the correlation of mass transfer in ducts is the blowing parameter, b. For many ducts a reasonable engineering approximation for the conductance is obtained from a 1-D analysis, as observed for many external flow problems. For large (negative or positive) values of b, a 1-D analysis is not appropriate, however the g/g^* data still compress on a single b-curve for the three geometries considered in this study.

Appendix A. Theoretical considerations

Berman's [2] equations may be written as follows:

$$\frac{u}{u_b} = \frac{3}{2}\left[1-\left(\frac{y}{H}\right)^2\right]\left[1+\frac{Re_w}{420}\left(2-7\left(\frac{y}{H}\right)^2-7\left(\frac{y}{H}\right)^4\right)\right] \tag{A.1}$$

$$\frac{v}{v_w} = \frac{y}{2H}\left[3-\left(\frac{y}{H}\right)^2\right]+\frac{Re_w}{280}\left(\frac{y}{H}\right)\left[2-3\left(\frac{y}{H}\right)+\left(\frac{y}{H}\right)^6\right] \tag{A.2}$$

where $u_b(x) = u_b(0) - v_w x/H$ is the local bulk velocity. Since $c_f^* = 24/Re$, the friction coefficient is obtained as

$$\frac{c_f}{c_f^*} = \left(1-\frac{Re_w}{35}\right) = \left(1-\frac{3}{35}b\right) \tag{A.3}$$

In the limit $Re_w \to 0$, the simplified form of Berman's equations is obtained,

$$\frac{u}{\bar{u}} = \frac{3}{2}\left[1 - \left(\frac{y}{H}\right)^2\right] \tag{A.4}$$

$$\frac{v}{v_w} = \frac{y}{2H}\left[3 - \left(\frac{y}{H}\right)^2\right] \tag{A.5}$$

Sherwood et al. [8,9] considered numerical solutions to the equation;

$$\rho u\frac{\partial \phi}{\partial x} + \rho v\frac{\partial \phi}{\partial y} = \frac{\partial}{\partial y}\Gamma\frac{\partial \phi}{\partial y} \tag{A.6}$$

These were obtained as

$$\phi = \sum_{n=0}^{\infty} B_n Y_n\left[1 - \frac{v_w}{u_b(0)}\frac{x}{H}\right]^{(2/3\beta_n - 1)} \tag{A.7}$$

Values of $\beta_n, Y_n(y/H)$ and B_n are given in [16] for $Pe_w = -2.0$, -3.7 and -14.8. Dresner [17] suggests that in the entrance region of the duct, near the wall, Eqs. (A.4) and (A.5) may be expanded in a Taylor series about $y = H$, i.e., $u/\bar{u} = 3(1 - y/H)$, $v/v_w = y/H$. Substitution into Eq. (A.6) yields,

$$\eta\frac{\partial \tilde{\phi}}{\partial \xi} - \frac{\partial \tilde{\phi}}{\partial \eta} = \frac{\partial^2 \tilde{\phi}}{\partial \eta^2} \tag{A.8}$$

where $\tilde{\phi} = (\phi - \phi_w)/(\phi_w - \phi_t)$, $\xi = \frac{1}{3}(v_w/\bar{u}_0)(4x/D_h)\times Pe_w^2$, and $\eta = Pe_w(1 - y/H)$. The solution is of the form $\tilde{\phi} = \tilde{\phi}(\xi, \eta)$. Since $B = \tilde{\phi}(\phi = \phi_b)$ is not a function of η; $B = B(\xi)$ or $\Phi = \Phi(\xi)$, alone. In practice there may be some deviation in the velocity profile, and the data may not compress onto a single characteristic between the entrance and fully-developed zones.

References

[1] D.B. Spalding, A standard formulation of the steady convective mass transfer problem, Int. J. Heat Mass Transfer 1 (1960) 192–207.

[2] A.S. Berman, Laminar flow in channels with porous walls, J. Appl. Phys. 24 (9) (1953) 1232–1235.

[3] J. Jorne, Mass transfer in laminar flow channel with porous wall, J. Electrochem. Soc. 129 (8) (1982) 1727–1733.

[4] P. Lessner, J.S. Newman, Hydrodynamics and mass-transfer in a porous-wall channel, J. Electrochem. Soc. 131 (8) (1984) 1828–1831.

[5] G.D. Raithby, D.C. Knudsen, Hydrodynamic development in a duct with suction and blowing, J. Appl. Mech. (Trans. ASME) 41 (1974) 892–902.

[6] S.K. Karode, Laminar flow in channels with porous walls, revisited, J. Membr. Sci. 191 (1) (2001) 237–241.

[7] S. Chellam, M.R. Wiesner, C. Dawson, Laminar-flow in porous ducts, Rev. Chem. Eng. 11 (1) (1995) 53–99.

[8] T.K. Sherwood, P.L.T. Brian, R.E. Fisher, L. Dressner, Salt concentration at phase boundaries, Ind. Eng. Chem. Fundam. 4 (1965) 113–118.

[9] T.K. Sherwood, P.L.T. Brian, R.E. Fisher, Salt concentration at phase boundaries in desalination processes, Desalination Research Laboratory Report 295-1, Massachusetts Institute of Technology, Cambridge, Massachusetts, August 1963.

[10] L. Dressner, Boundary layer buildup in the demineralization of salt water by reverse osmosis, ORNL-3621, Oak Ridge National Laboratory, Oak Ridge, Tennessee, May 1964.

[11] G.D. Raithby, Heat transfer in tubes and ducts with wall mass transfer, Canadian J. Chem. Eng. 50 (1972) 456–461.

[12] G.D. Raithby, Laminar heat transfer in the thermal entrance region of circular tubes and two-dimensional rectangular ducts with wall suction and injection, Int. J. Heat Mass Transfer 14 (1971) 223–243.

[13] R.M. Terrill, Heat transfer in laminar flow between parallel porous plates, Int. J. Heat Mass Transfer 8 (1965) 1491–1497.

[14] L.C. Chow, A. Campo, C.L. Tien, Heat-transfer characteristics for laminar-flow between parallel plates with suction, Int. J. Heat Mass Transfer 23 (5) (1980) 740–743.

[15] F. Bellucci, A. Pozzi, Numerical and analytical solutions for concentration polarization in continuous reverse-osmosis processes, Quad. Ing. Chim. Ital. 16 (3) (1980) 30–34.

[16] V. Geraldes, V. Semiao, M.N. Pinho, Numerical modelling of mass transfer in slits with semi-permeable membrane walls, Eng. Comput. 17 (3) (2000) 192–217.

[17] D.E. Wiley, D.F. Fletcher, Computational fluid dynamics modelling of flow and permeation for pressure-driven membrane processes, Desalination 145 (1) (2002) 183–186.

[18] D.E. Wiley, D.F. Fletcher, Techniques for computational fluid dynamics modelling of flow in membrane channels, J. Membr. Sci. 211 (2003) 127–137.

[19] J. Yuan, M. Rokni, B. Sundén, Simulation of fully developed laminar heat and mass transfer in fuel cell ducts with different cross-sections, Int. J. Heat Mass Transfer 55 (2001) 4047–4058.

[20] S.V. Patankar, Numerical Heat Transfer and Fluid Flow, Hemisphere, New York, 1980.

[21] S.B. Beale, D.B. Spalding, Numerical study of fluid flow and heat transfer in tube banks with stream-wise periodic boundary conditions, Trans. CSME 22 (4A) (1998) 394–416.

[22] R.K. Shah, A.L. London, Laminar flow forced convection in ducts, in: T.F. Irvine, J.P. Hartnett (Eds.), Advances in Heat Transfer, Academic Press, New York, 1978, p. 206.

[23] S.B. Beale, Some aspects of mass transfer within the passages of fuel cells, in: Proceedings 1st International Fuel Cell Science, Engineering and Technology, ASME, 2003, pp. 293–299.